EUROPEAN ORGANIZATION FOR NUCLEAR RESEARCH

CERN-PPE/94-68
April 25, 1994

Measurement of the Inclusive $\mathrm{b} \rightarrow \tau\nu\mathrm{X}$ Branching Ratio

The L3 Collaboration

ABSTRACT

Using the L3 detector, the branching ratio $\mathrm{BR}(\mathrm{b} \rightarrow \tau\nu\mathrm{X})$ has been measured using a sample of $\mathrm{Z} \rightarrow \mathrm{b\bar{b}}$ events tagged by high momentum and high transverse momentum leptons in one hemisphere and with missing energy in the opposite hemisphere. From a sample of 948 000 hadronic events we find

$$\mathrm{BR}(\mathrm{b} \rightarrow \tau\nu\mathrm{X}) = (2.4 \pm 0.7\,(\mathrm{stat.}) \pm 0.8\,(\mathrm{syst.}))\%.$$

(Submitted to Phys. Lett. B)

Introduction

The measurement of the branching ratio BR(b $\rightarrow \tau\nu$X) is an interesting test of the Standard Model (SM) [1], which predicts a value of $(2.3 \pm 0.3)\%$ [2]. Supersymmetric extensions [3] can allow larger values (up to 20%), due to additional contributions coming from the exchange of charged Higgs bosons [4]. A previous measurement was reported in reference 5.

The main signature of the b $\rightarrow \tau\nu$X, $\tau \rightarrow \nu$X decay chain is the large missing energy associated with the production of the two neutrinos. The main sources of background are hadronic events which have a large missing energy due to the finite resolution of the detector, and semileptonic b and c decays to electrons or muons with highly energetic neutrinos. To reduce these backgrounds an enriched sample of b $\rightarrow \tau\nu$X candidates was selected in two steps. First, a sample of Z $\rightarrow$ b$\bar{\text{b}}$ events was obtained using high momentum and high transverse momentum electrons and muons as tags. The events were then required to have large missing energy and no electron or muon candidates in the hemisphere opposite to the tagging lepton.

The L3 Detector

The L3 detector [6] measures e, γ, μ and jets with high precision. The central tracking chamber is a Time Expansion Chamber (TEC) consisting of two coaxial cylindrical drift chambers; the electromagnetic calorimeter is composed of bismuth germanate (BGO) crystals; hadronic energy depositions are measured by a uranium-proportional wire chamber sampling calorimeter surrounding the BGO; scintillator timing counters are located between the electromagnetic and hadronic calorimeters. The muon spectrometer, located outside the hadron calorimeter, consists of three layers of drift chambers measuring the muon trajectory in both the bending and the non-bending planes. All subdetectors are installed inside a 12 m diameter solenoid which provides a uniform field of 0.5 T along the beam direction.

Because this analysis relies on missing energy measurements, only data collected during periods in which all subdetectors were fully operational was used in this analysis.

Event Selection

Hadronic events were selected by requiring: $0.4 < E_{vis} / \sqrt{s} < 1.5$, where E_{vis} is the total calorimetric energy observed in the detector; $N_{clus} > 13$, where N_{clus} is the number of energy clusters reconstructed in the calorimeters; and at least one charged track. From the 1991 and 1992 data a total sample of 948 067 events was selected. In order for the events to be well contained in the central region of the detector, they were required to have $|\cos\theta_t| < 0.72$, where θ_t is the angle between the thrust axis of the event and the electron beam direction.

An enriched sample of Z $\rightarrow$ b$\bar{\text{b}}$ events was obtained by requiring at least one lepton candidate with high momentum and high transverse momentum with respect to the nearest jet [7]. Electron candidates were found by associating a cluster in the BGO barrel calorimeter ($|\cos\theta| < 0.71$), whose lateral shape was consistent with an electromagnetic shower, with a track in the central tracking chamber. The BGO cluster and the TEC track were required to match in azimuth within 8 mrad. To reduce hadronic background, the energy in the hadron calorimeter behind the electromagnetic cluster was required to be less than 4 GeV . To reject energetic π°'s and photons close to a charged track, the ratio of the BGO energy to the momentum of the TEC track was required to satisfy $E / p < 2$.

Muon candidates were identified and measured in the muon chamber system within a fiducial volume $|\cos\theta| < 0.72$. A muon track was required to have track segments reconstructed in at least two out of three $r\phi$ layers of muon chambers and at least one of the two z layers and to point to the interaction region. These requirements are very effective in rejecting hadronic punchthrough and decay muons.

Selected lepton candidates were required to have a momentum larger than 4 GeV for muons and 3 GeV for electrons. The momentum transverse to the nearest jet, $p_\perp$, was required to be greater than 1 GeV both for electrons and muons (the measured energy of the lepton was excluded in the calculation of the jet direction).

After applying these selection criteria, 15761 events were tagged by an electron and 19429 by a muon, giving

$$N_{tag} = 35190.$$

To detect the $\mathrm{b} \to \tau\nu\mathrm{X}$ signal, each event was divided into two hemispheres defined by the plane orthogonal to the thrust axis. The visible energy, E_{vis}^{hemi}, in the hemisphere opposite to the one containing the tagging lepton (hereafter referred to as the signal hemisphere) was measured. The missing energy in this hemisphere was defined to be

$$E_{miss}^{hemi} = \sqrt{s}\,/\,2 - E_{vis}^{hemi}.$$

To reject events with electrons or muons in this hemisphere, looser identification criteria were applied to search for candidates: the minimum momentum required of either a muon or an electron candidate was 2 GeV and, for electron candidates, the cut on azimuthal angle between the BGO cluster and the TEC track was relaxed to 20 mrad. The momentum spectra of these electron and muon candidates in the signal hemisphere in the rejected events are shown in Figure 1.

The $\mathrm{b} \to \tau\nu\mathrm{X}$ fraction was enriched by requiring

$$E_{miss}^{hemi} > 14 \ \mathrm{GeV}.$$

Reducing the value of this cut degrades the signal to background ratio owing to the contributions of light quarks and nonleptonic b decays. The final number of events surviving all cuts is

$$N_{obs} = 1032.$$

Analysis Method

The total number of $\mathrm{b} \to \tau\nu\mathrm{X}$ events in the sample of tagged events was calculated using

$$N_\tau = \frac{N_{obs} - \epsilon_{bg} N_{tag}}{\epsilon_\tau - \epsilon_{bg}},$$

where ϵ_τ and ϵ_{bg} are the fractions of signal and background events in the sample of tagged events which passed all cuts. $\mathrm{BR}(\mathrm{b} \to \tau\nu\mathrm{X})$ can be derived from:

$$\mathrm{BR}(\mathrm{b} \to \tau\nu\mathrm{X}) = \frac{N_\tau}{N_{\mathrm{b\bar{b}}}} = \frac{N_\tau}{\pi_{\mathrm{b\bar{b}}} N_{tag}},$$

where $N_{\mathrm{b\bar{b}}}$ is the total number of $\mathrm{b\bar{b}}$ events in the tagged sample and $\pi_{\mathrm{b\bar{b}}}$ is the purity of this sample.

In order to determine the various acceptances for signal and backgrounds, more than 2 million Monte Carlo (MC) events were generated with the Lund parton shower program, JETSET 7.3 [8], using $\mathrm{BR}(\mathrm{b} \to \ell\nu\mathrm{X}) = 0.110 \pm 0.005$ [9], where $\ell = \mathrm{e}, \mu$ and $\mathrm{BR}(\mathrm{D_s} \to \tau\nu) = 0.037 \pm 0.023$ [10]. The latter process, having the same kinematical signature as the signal, constitutes a small but irreducible background. The events were passed through the complete L3 detector simulation [11] which includes the effects of energy loss, multiple scattering, interactions and decays in the detector materials. Dead or noisy BGO crystals, and inefficiencies in the TEC and muon chambers were simulated using the time-dependent detector status determined using the data. With the above simulation the purity of the tagged sample was found to be $\pi_{\mathrm{b\bar{b}}} = 73.7\%$.

The measurement of E_{miss}^{hemi} was checked for systematic biases by studying the missing energy in the tagging hemisphere, where the contribution of the signal is expected to be negligible. In the region of positive missing energy, the distribution of this quantity is similar to that in the opposite hemisphere, as the main contribution in both cases comes from semileptonic b decays. The distributions of missing energy in the tagging hemisphere for data and MC events are compared in Figure 2, showing very good agreement for positive missing energies. For negative values, corresponding to large values of the visible energy, a difference is observed. This could be corrected by applying an energy dependent scale factor to the missing energy, but it should be noted that no scale factor was necessary for $E_{miss}^{hemi} > 2 \ \mathrm{GeV}$. However, a shift of up to 200 MeV cannot be excluded and this uncertainty was included in the systematic error. The corrected E^{hemi}_{miss} distribution for the events without a second lepton, is shown in Figure 3 for data and MC. The same figure shows the expected contribution of $\mathrm{b} \to \tau\nu\mathrm{X}$ events, assuming the SM value for the branching ratio.

In Figure 4, the data are compared with the predicted background in the E^{hemi}_{miss} range where the signal is expected to appear. The clear excess visible in the data above about 10 GeV is interpreted as the $\mathrm{b} \to \tau\nu\mathrm{X}$ signal.

Results

After all cuts, the efficiency for the signal, obtained from the MC, is

$$\epsilon_\tau = 21.1\%,$$

while the fraction of the background events passing all cuts was found to be

$$\epsilon_{bg} = 2.6\%.$$

Using the formulæ from the previous section, the branching ratio is determined to be:

$$\mathrm{BR}(\mathrm{b} \to \tau\nu\mathrm{X}) = (2.4 \pm 0.7)\%.$$

This corresponds to 133 observed signal events calculated from $[N_{obs} - \epsilon_{bg}(N_{tag} - N_\tau)]$.

The main contribution to the systematic error comes from the background subtraction. The major instrumental uncertainties are due to the lepton candidate criteria in the signal hemisphere and to the cut on E^{hemi}_{miss}.

In order to study the systematic uncertainty introduced by the rejection of events with a second lepton the sample of tagged events has been divided into three classes: events without a second lepton, events with an additional electron and events with an additional muon. The comparison of the size of the three classes in MC and data showed that the fraction of events in the first class are reproduced at the 1% level, events in the second class at the 7% level and events of the third class at the 0.5% level. The effect on $\mathrm{BR}(\mathrm{b} \to \tau\nu\mathrm{X})$ can then be evaluated by varying the number of events without a second lepton found in the final sample by 1%. An alternative estimate was obtained by varying the number of events with an additional electron found in the final sample by 7% and those with an additional muon by 0.5% and combining the two contributions in quadrature. The largest error on $\mathrm{BR}(\mathrm{b} \to \tau\nu\mathrm{X})$, 0.3%, is given by the second estimate. Another estimate of the same error was obtained by varying, separately for electron and muon candidates, the momentum cut in the interval from 2 to 3 GeV. This method leads to a systematic uncertainty of 0.2%. The branching ratio can also be determined without any veto on additional leptons, but with a larger dependence of the background on $\mathrm{BR}(\mathrm{b} \to \ell\nu\mathrm{X})$. This results in a change of $\mathrm{BR}(\mathrm{b} \to \tau\nu\mathrm{X})$ of only 0.15%. Taking the above four studies a conservative uncertainty of 0.3% was attributed to the effect of the lepton cuts.

The uncertainty coming from the E^{hemi}_{miss} cut has been evaluated by varying the value of this cut in the range of $\pm$ 2 GeV around the nominal value of 14 GeV. This leads to a systematic error of 0.3%. Below this range the systematic error due to the background subtraction increases significantly, while above this range the statistical significance decreases. This uncertainty can also be estimated by scaling the E^{hemi}_{miss} calculated in the MC by the maximum scale shift of 200 MeV allowed by the comparison of the corresponding distributions for data and MC in the tagged hemisphere, as discussed above. This leads to a change of 0.4% in the value of $\mathrm{BR}(\mathrm{b} \to \tau\nu\mathrm{X})$, in agreement with the previous estimation.

The error on the purity of the tagged sample, $\pi_{\mathrm{b\bar{b}}}$, arises from uncertainties in the tagging efficiency for $\mathrm{b\bar{b}}$ events and in the fraction of events coming from lighter quarks. Conservatively allowing a variation of 3% and 5% in these values respectively, results in an uncertainty of 0.1% in the value of $\mathrm{BR}(\mathrm{b} \to \tau\nu\mathrm{X})$.

The value of $\mathrm{BR}(\mathrm{b} \to \tau\nu\mathrm{X})$ also depends on the decay model used to estimate the background: the dominant uncertainty in the background comes from the semileptonic b decays. The variation of $\mathrm{BR}(\mathrm{b} \to \ell\nu\mathrm{X})$ by one standard deviation around the central value used in the simulation results in an error of 0.5%. The remaining uncertainty coming from the subtraction of $D_s \to \tau\nu$ decays has also been evaluated by changing the value of the branching ratio used in the simulation by one standard deviation, and leads to an uncertainty of 0.2%.

Monte Carlo statistics	$0.4\,\%$
Lepton efficiency	$0.3\,\%$
Cut on E_{miss}^{hemi}	$0.3\,\%$
Purity of $b\bar{b}$ sample	$0.1\,\%$
$BR(D_s \to \tau\nu)$	$0.2\,\%$
$BR(b \to \ell\nu X)$	$0.5\,\%$

Table 1: Contributions to the systematic error on $BR(b \to \tau\nu X)$.

The various systematic errors on $BR(b \to \tau\nu X)$ are summarized in Table 1. Our measurement can then be written as:

$$BR(b \to \tau\nu X) = (2.4 \pm 0.7\,(\mathrm{stat.}) \pm 0.6\,(\mathrm{syst.}) \pm 0.5\,(\mathrm{BR}))\%,$$

where the uncertainty due to $BR(b \to \ell\nu X)$ is given explicitly and the other systematic errors have been added in quadrature. The dependence of the result on the deviation of $BR(b \to \ell\nu X)$ from its central value is $BR(b \to \tau\nu X) = \{2.4 + 0.98 \cdot [11.0 - BR(b \to \ell\nu X)]\}\ \%$, where $BR(b \to \ell\nu X)$ is given in percent. Combining all the systematic errors in quadrature, our final result is:

$$BR(b \to \tau\nu X) = (2.4 \pm 0.7\,(\mathrm{stat.}) \pm 0.8\,(\mathrm{syst.}))\%.$$

This value is in good agreement with the Standard Model prediction and with the previous measurement. There is no indication of a large enhancement as allowed in some theoretical models.

Acknowledgments

We wish to express our gratitude to the CERN accelerator divisions for the excellent performance of the LEP machine. We acknowledge the contributions of all the engineers and technicians who have participated in the construction and maintenance of this experiment.

The L3 Collaboration:

M.Acciarri,[26] A.Adam,[44] O.Adriani,[16] M.Aguilar-Benitez,[25] S.Ahlen,[10] J.Alcaraz,[17] A.Aloisio,[28] G.Alverson,[11] M.G.Alviggi,[28] G.Ambrosi,[33] Q.An,[18] H.Anderhub,[47] A.L.Anderson,[15] V.P.Andreev,[37] T.Angelescu,[12] L.Antonov,[41] D.Antreasyan,[8] G.Alkhazov,[37] P.Arce,[25] A.Arefiev,[27] T.Azemoon,[3] T.Aziz,[9] P.V.K.S.Baba,[18] P.Bagnaia,[36] J.A.Bakken,[35] L.Baksay,[43] R.C.Ball,[3] S.Banerjee,[9] K.Banicz,[44] R.Barillère,[17] L.Barone,[36] A.Baschirotto,[26] R.Battiston,[33] A.Bay,[19] F.Becattini,[16] U.Becker,[15] F.Behner,[47] Gy.L.Bencze,[13] J.Berdugo,[25] P.Berges,[15] B.Bertucci,[33] B.L.Betev,[41,47] M.Biasini,[33] A.Biland,[47] G.M.Bilei[33] R.Bizzarri,[36] J.J.Blaising,[4] G.J.Bobbink,[17,2] R.Bock,[1] A.Böhm,[1] B.Borgia,[36] D.Bourilkov,[47] M.Bourquin,[19] D.Boutigny,[17] B.Bouwens,[2] E.Brambilla,[28] J.G.Branson,[38] V.Brigljevic,[47] I.C.Brock,[34] M.Brooks,[23] A.Bujak,[44] J.D.Burger,[15] W.J.Burger,[19] C.Burgos,[25] J.Busenitz,[43] A.Buytenhuijs,[30] A.Bykov,[37] X.D.Cai,[18] M.Capell,[15] M.Caria,[33] G.Carlino,[28] A.M.Cartacci,[16] J.Casaus,[25] R.Castello,[26] N.Cavallo,[28] M.Cerrada,[25] F.Cesaroni,[36] M.Chamizo,[25] Y.H.Chang,[49] U.K.Chaturvedi,[18] M.Chemarin,[24] A.Chen,[49] C.Chen,[6] G.Chen,[6,47] G.M.Chen,[6] H.F.Chen,[20] H.S.Chen,[6] M.Chen,[15] G.Chiefari,[28] C.Y.Chien,[5] M.T.Choi,[42] S.Chung,[15] C.Civinini,[16] I.Clare,[15] R.Clare,[15] T.E.Coan,[23] H.O.Cohn,[31] G.Coignet,[4] N.Colino,[17] A.Contin,[8] S.Costantini,[36] F.Cotorobai,[12] B.de la Cruz,[25] X.T.Cui,[18] X.Y.Cui,[18] T.S.Dai,[15] R.D'Alessandro,[16] R.de Asmundis,[28] A.Degré,[4] K.Deiters,[45] E.Dénes,[13] P.Denes,[35] F.DeNotaristefani,[36] D.DiBitonto,[43] M.Diemoz,[36] H.R.Dimitrov,[41] C.Dionisi,[36] M.Dittmar,[47] L.Djambazov,[47] M.T.Dova,[18,♯] E.Drago,[28] D.Duchesneau,[19] P.Duinker,[2] I.Duran,[39] S.Easo,[33] H.El Mamouni,[24] A.Engler,[34] F.J.Eppling,[15] F.C.Erné,[2] P.Extermann,[19] R.Fabbretti,[45] M.Fabre,[45] S.Falciano,[36] S.J.Fan,[40] A.Favara,[16] J.Fay,[24] M.Felcini,[47] T.Ferguson,[34] D.Fernandez,[25] G.Fernandez,[25] F.Ferroni,[36] H.Fesefeldt,[1] E.Fiandrini,[33] J.H.Field,[19] F.Filthaut,[30] P.H.Fisher,[5] G.Forconi,[15] L.Fredj,[19] K.Freudenreich,[47] M.Fukushima,[15] M.Gailloud,[22] Yu.Galaktionov,[27,15] E.Gallo,[16] S.N.Ganguli,[9] P.Garcia-Abia,[25] S.Gentile,[36] J.Gerald,[5] N.Gheordanescu,[12] S.Giagu,[36] S.Goldfarb,[22] Z.F.Gong,[20] E.Gonzalez,[25] A.Gougas,[5] D.Goujon,[19] G.Gratta,[32] M.Gruenewald,[17] C.Gu,[18] M.Guanziroli,[18] J.K.Guo,[40] V.K.Gupta,[35] A.Gurtu,[9] H.R.Gustafson,[3] L.J.Gutay,[44] A.Hasan,[18] D.Hauschildt,[2] C.F.He,[40] J.T.He,[6] T.Hebbeker,[7] M.Hebert,[38] A.Hervé,[17] K.Hilgers,[1] H.Hofer,[47] H.Hoorani,[19] S.R.Hou,[49] G.Hu,[18] G.Q.Hu,[40] B.Ille,[24] M.M.Ilyas,[18] V.Innocente,[17] H.Janssen,[4] B.N.Jin,[6] L.W.Jones,[3] P.de Jong,[15] I.Josa-Mutuberria,[17] A.Kasser,[22] R.A.Khan,[18] Yu.Kamyshkov,[31] P.Kapinos,[46] J.S.Kapustinsky,[23] Y.Karyotakis,[17] M.Kaur,[18] S.Khokhar,[18] M.N.Kienzle-Focacci,[19] D.Kim,[5] J.K.Kim,[42] S.C.Kim,[42] Y.G.Kim,[42] W.W.Kinnison,[23] A.Kirkby,[32] D.Kirkby,[32] S.Kirsch,[46] W.Kittel,[30] A.Klimentov,[15,27] A.C.König,[30] E.Koffeman,[2] O.Kornadt,[1] V.Koutsenko,[15,27] A.Koulbardis,[37] R.W.Kraemer,[34] T.Kramer,[15] V.R.Krastev,[41,33] W.Krenz,[1] H.Kuijten,[30] K.S.Kumar,[14] A.Kunin,[15,27] P.Ladron de Guevara,[25] G.Landi,[16] D.Lanske,[1] S.Lanzano,[28] A.Lebedev,[15] P.Lebrun,[24] P.Lecomte,[47] P.Lecoq,[17] P.Le Coultre,[47] D.M.Lee,[23] J.S.Lee,[42] K.Y.Lee,[42] I.Leedom,[11] C.Leggett,[3] J.M.Le Goff,[17] R.Leiste,[46] M.Lenti,[16] E.Leonardi,[36] P.Levtchenko,[37] C.Li,[20,18] P.J.Li,[40] J.Y.Liao,[40] W.T.Lin,[49] Z.Y.Lin,[20] F.L.Linde,[2] B.Lindemann,[1] L.Lista,[28] Y.Liu,[18] W.Lohmann,[46] E.Longo,[36] W.Lu,[32] Y.S.Lu,[6] J.M.Lubbers,[17] K.Lübelsmeyer,[1] C.Luci,[36] D.Luckey,[8,15] L.Ludovici,[36] L.Luminari,[36] W.Lustermann,[45] W.G.Ma,[20] M.MacDermott,[47] L.Malgeri,[36] R.Malik,[18] A.Malinin,[27] C.Maña,[25] M.Maolinbay,[47] P.Marchesini,[47] F.Marion,[4] A.Marin,[10] J.P.Martin,[24] F.Marzano,[36] G.G.G.Massaro,[2] K.Mazumdar,[9] P.McBride,[14] T.McMahon,[44] D.McNally,[38] M.Merk,[34] L.Merola,[28] M.Meschini,[16] W.J.Metzger,[30] Y.Mi,[22] A.Mihul,[12] G.B.Mills,[23] Y.Mir,[18] G.Mirabelli,[36] J.Mnich,[1] M.Möller,[1] B.Monteleoni,[16] R.Morand,[4] S.Morganti,[36] N.E.Moulai,[18] R.Mount,[32] S.Müller,[1] E.Nagy,[13] M.Napolitano,[28] F.Nessi-Tedaldi,[47] H.Newman,[32] M.A.Niaz,[18] A.Nippe,[1] H.Nowak,[46] G.Organtini,[36] D.Pandoulas,[1] S.Paoletti,[36] P.Paolucci,[28] G.Pascale,[36] G.Passaleva,[16,33] S.Patricelli,[28] T.Paul,[5] M.Pauluzzi,[33] C.Paus,[1] F.Pauss,[47] Y.J.Pei,[1] S.Pensotti,[26] D.Perret-Gallix,[4] J.Perrier,[19] A.Pevsner,[5] D.Piccolo,[28] M.Pieri,[17] J.C.Pinto,[34] P.A.Piroué,[35] F.Plasil,[31] V.Plyaskin,[27] M.Pohl,[47] V.Pojidaev,[27,16] H.Postema,[15] Z.D.Qi,[40] J.M.Qian,[3] K.N.Qureshi,[18] R.Raghavan,[9] G.Rahal-Callot,[47] P.G.Rancoita,[26] M.Rattaggi,[26] G.Raven,[2] P.Razis,[29] K.Read,[31] M.Redaelli,[26] D.Ren,[47] Z.Ren,[18] M.Rescigno,[36] S.Reucroft,[11] A.Ricker,[1] S.Riemann,[46] B.C.Riemers,[44] O.Rind,[3] H.A.Rizvi,[18] S.Ro,[42] A.Robohm,[47] F.J.Rodriguez,[25] B.P.Roe,[3] M.Röhner,[1] S.Röhner,[1] L.Romero,[25] S.Rosier-Lees,[4] R.Rosmalen,[30] Ph.Rosselet,[22] W.van Rossum,[2] S.Roth,[1] A.Rubbia,[15] J.A.Rubio,[17] H.Rykaczewski,[47] M.Sachwitz,[46] J.Salicio,[17] J.M.Salicio,[25] E.Sanchez,[25] G.S.Sanders,[23] A.Santocchia,[33] M.E.Sarakinos,[44] G.Sartorelli,[8,18] M.Sassowsky,[1] G.Sauvage,[4] C.Schäfer,[1] V.Schegelsky,[37] D.Schmitz,[1] P.Schmitz,[1] M.Schneegans,[4] N.Scholz,[47] H.Schopper,[48] D.J.Schotanus,[30] S.Shotkin,[15] H.J.Schreiber,[46] J.Shukla,[34] R.Schulte,[1] K.Schultze,[1] J.Schwenke,[1] G.Schwering,[1] C.Sciacca,[28] I.Scott,[14] R.Sehgal,[18] P.G.Seiler,[45] J.C.Sens,[17,2] L.Servoli,[33] I.Sheer,[38] D.Z.Shen,[40] S.Shevchenko,[32] X.R.Shi,[32] E.Shumilov,[27] V.Shoutko,[27] D.Son,[42] A.Sopczak,[17] V.Soulimov,[28] C.Spartiotis,[21] T.Spickermann,[1] P.Spillantini,[16] M.Steuer,[8,15] D.P.Stickland,[35] F.Sticozzi,[15] H.Stone,[35] K.Strauch,[14] K.Sudhakar,[9] G.Sultanov,[18] L.Z.Sun,[20,18] G.F.Susinno,[19] H.Suter,[47] J.D.Swain,[18] A.A.Syed,[30] X.W.Tang,[6] L.Taylor,[11] Samuel C.C.Ting,[15] S.M.Ting,[15] O.Toker,[33] M.Tonutti,[1] S.C.Tonwar,[9] J.Tóth,[13] G.Trowitzsch,[46] A.Tsaregorodtsev,[37] G.Tsipolitis,[34] C.Tully,[35] T.Tuuva,[21] J.Ulbricht,[47] L.Urbán,[13] U.Uwer,[1] E.Valente,[36] R.T.Van de Walle,[30] I.Vetlitsky,[27] G.Viertel,[47] P.Vikas,[18] U.Vikas,[18] M.Vivargent,[4] H.Vogel,[34] H.Vogt,[46] I.Vorobiev,[14,27] A.A.Vorobyov,[37] An.A.Vorobyov,[37] L.Vuilleumier,[22] M.Wadhwa,[4] W.Wallraff,[1] J.C.Wang,[15] C.R.Wang,[20] X.L.Wang,[20] Y.F.Wang,[15] Z.M.Wang,[18,20] A.Weber,[1] J.Weber,[47] R.Weill,[22] J.Wenninger,[19] M.White,[15] C.Willmott,[25] F.Wittgenstein,[17] D.Wright,[35] S.X.Wu,[18] S.Wynhoff,[1] B.Wysłouch,[15] Y.Y.Xie,[40] Z.Z.Xu,[20] Z.L.Xue,[40] D.S.Yan,[40] B.Z.Yang,[20] C.G.Yang,[6] G.Yang,[18] X.Y.Yao,[6] C.H.Ye,[18] J.B.Ye,[20] Q.Ye,[18] S.C.Yeh,[49] Z.W.Yin,[40] J.M.You,[18] N.Yunus,[18] M.Yzerman,[2] C.Zaccardelli,[32] P.Zemp,[47] M.Zeng,[18] Y.Zeng,[1] D.H.Zhang,[2] Z.P.Zhang,[20,18] B.Zhou,[10] G.J.Zhou,[6] J.F.Zhou,[1] R.Y.Zhu,[32] A.Zichichi,[8,17,18] B.C.C.van der Zwaan.[2]

1 I. Physikalisches Institut, RWTH, D-52056 Aachen, FRG[§]
III. Physikalisches Institut, RWTH, D-52056 Aachen, FRG[§]
2 National Institute for High Energy Physics, NIKHEF, NL-1009 DB Amsterdam, The Netherlands
3 University of Michigan, Ann Arbor, MI 48109, USA
4 Laboratoire d'Annecy-le-Vieux de Physique des Particules, LAPP,IN2P3-CNRS, BP 110, F-74941 Annecy-le-Vieux CEDEX, France
5 Johns Hopkins University, Baltimore, MD 21218, USA
6 Institute of High Energy Physics, IHEP, 100039 Beijing, China
7 Humboldt University, D-10099 Berlin, FRG
8 INFN-Sezione di Bologna, I-40126 Bologna, Italy
9 Tata Institute of Fundamental Research, Bombay 400 005, India
10 Boston University, Boston, MA 02215, USA
11 Northeastern University, Boston, MA 02115, USA
12 Institute of Atomic Physics and University of Bucharest, R-76900 Bucharest, Romania
13 Central Research Institute for Physics of the Hungarian Academy of Sciences, H-1525 Budapest 114, Hungary[‡]
14 Harvard University, Cambridge, MA 02139, USA
15 Massachusetts Institute of Technology, Cambridge, MA 02139, USA
16 INFN Sezione di Firenze and University of Florence, I-50125 Florence, Italy
17 European Laboratory for Particle Physics, CERN, CH-1211 Geneva 23, Switzerland
18 World Laboratory, FBLJA Project, CH-1211 Geneva 23, Switzerland
19 University of Geneva, CH-1211 Geneva 4, Switzerland
20 Chinese University of Science and Technology, USTC, Hefei, Anhui 230 029, China
21 SEFT, Research Institute for High Energy Physics, P.O. Box 9, SF-00014 Helsinki, Finland
22 University of Lausanne, CH-1015 Lausanne, Switzerland
23 Los Alamos National Laboratory, Los Alamos, NM 87544, USA
24 Institut de Physique Nucléaire de Lyon, IN2P3-CNRS,Université Claude Bernard, F-69622 Villeurbanne Cedex, France
25 Centro de Investigaciones Energeticas, Medioambientales y Tecnologicas, CIEMAT, E-28040 Madrid, Spain
26 INFN-Sezione di Milano, I-20133 Milan, Italy
27 Institute of Theoretical and Experimental Physics, ITEP, Moscow, Russia
28 INFN-Sezione di Napoli and University of Naples, I-80125 Naples, Italy
29 Department of Natural Sciences, University of Cyprus, Nicosia, Cyprus
30 University of Nymegen and NIKHEF, NL-6525 ED Nymegen, The Netherlands
31 Oak Ridge National Laboratory, Oak Ridge, TN 37831, USA
32 California Institute of Technology, Pasadena, CA 91125, USA
33 INFN-Sezione di Perugia and Universitá Degli Studi di Perugia, I-06100 Perugia, Italy
34 Carnegie Mellon University, Pittsburgh, PA 15213, USA
35 Princeton University, Princeton, NJ 08544, USA
36 INFN-Sezione di Roma and University of Rome, "La Sapienza", I-00185 Rome, Italy
37 Nuclear Physics Institute, St. Petersburg, Russia
38 University of California, San Diego, CA 92093, USA
39 Dept. de Fisica de Particulas Elementales, Univ. de Santiago, E-15706 Santiago de Compostela, Spain
40 Shanghai Institute of Ceramics, SIC, Shanghai, China
41 Bulgarian Academy of Sciences, Institute of Mechatronics, BU-1113 Sofia, Bulgaria
42 Center for High Energy Physics, Korea Advanced Inst. of Sciences and Technology, 305-701 Taejon, Republic of Korea
43 University of Alabama, Tuscaloosa, AL 35486, USA
44 Purdue University, West Lafayette, IN 47907, USA
45 Paul Scherrer Institut, PSI, CH-5232 Villigen, Switzerland
46 DESY-Institut für Hochenergiephysik, D-15738 Zeuthen, FRG
47 Eidgenössische Technische Hochschule, ETH Zürich, CH-8093 Zürich, Switzerland
48 University of Hamburg, 22761 Hamburg, FRG
49 High Energy Physics Group, Taiwan, China
§ Supported by the German Bundesministerium für Forschung und Technologie
‡ Supported by the Hungarian OTKA fund under contract number 2970.
♯ Also supported by CONICET and Universidad Nacional de La Plata, CC 67, 1900 La Plata, Argentina

References

[1] S. L. Glashow, Nucl. Phys. **22** (1961) 579;
S. Weinberg, Phys. Rev. Lett. **19** (1967) 1264;
A. Salam, “Elementary Particle Theory”, Ed. N. Svartholm, Stockholm, “Almquist and Wiskell” (1968), 367.

[2] A. F. Falk, Z. Ligeti, M. Neubert and Y. Nir, Preprint CERN-TH/93-7124.

[3] R. Barbieri, Riv. Nuo. Cim. **11** (1988) 1.

[4] P. Krawczyk and S. Pokorski, Phys. Rev. Lett. **60** (1988) 182;
B. Grzadkowski and W. S. Hou, Phys. Lett. **B272** (1991) 383;
G. Isidori, Phys. Lett. **B298** (1992) 409.

[5] ALEPH Collab., D. Buskulic *et al.*, Phys. Lett. **B298** (1993) 479.

[6] L3 Collab., B. Adeva *et al.*, Nucl. Instrum. Methods **A 289** (1990) 35;
L3 Collab., O. Adriani *et al.*, Phys. Rep. **236** (1993) 1.

[7] O. Adriani *et al.*, Nucl. Instrum. Methods **A 302** (1991) 53.

[8] T. Sjöstrand, Comp. Phys. Comm. **39** (1986) 347;
T. Sjöstrand and M. Bengtsson, Comp. Phys. Comm. **43** (1987) 367.

[9] LEP average, calculated from:
L3 Collab., B. Adeva *et al.*, Phys. Lett. **B261** (1991) 177;
DELPHI Collab., P. Abreu *et al.*, Phys. Lett. **B301** (1993) 145;
OPAL Collab., R. Akers *et al.*, Z. Phys. **C 60** (1993) 199;
ALEPH Collab., D. Buskulic *et al.*, CERN-PPE/94-017, submitted to Z. Phys.

[10] WA75 Collab., S. Aoki *et al.*, Progr. Theor. Phys. **89** (1993) 131.

[11] The L3 detector simulation program is based on the GEANT program:
R. Brun *et al.*, “GEANT 3”, CERN report **DD/EE/84-1** (1984) (Revised), September 1987.
Hadronic interactions in the detector were modelled using GHEISHA:
H. Fesefeldt, RWTH Aachen report **PYTHIA 85/02** (1985).

Figure Captions

Figure 1. Momentum distributions of the a) electrons and b) muons found in the signal hemisphere for data and Monte Carlo.

Figure 2. Distributions of the missing energy in the tagging hemisphere for data and Monte Carlo.

Figure 3. Distributions of the missing energy in the signal hemisphere, E_{miss}^{hemi}, for data and Monte Carlo; the latter is corrected by the scale factor described in the text . The cross-hatched area corresponds to the expected contribution of b $\rightarrow$ $\tau\nu$X.

Figure 4. Distributions of E_{miss}^{hemi} for data and predicted backgrounds. The solid line shows the total background, while the dashed line shows the contributions from light quarks and nonleptonic b decays.

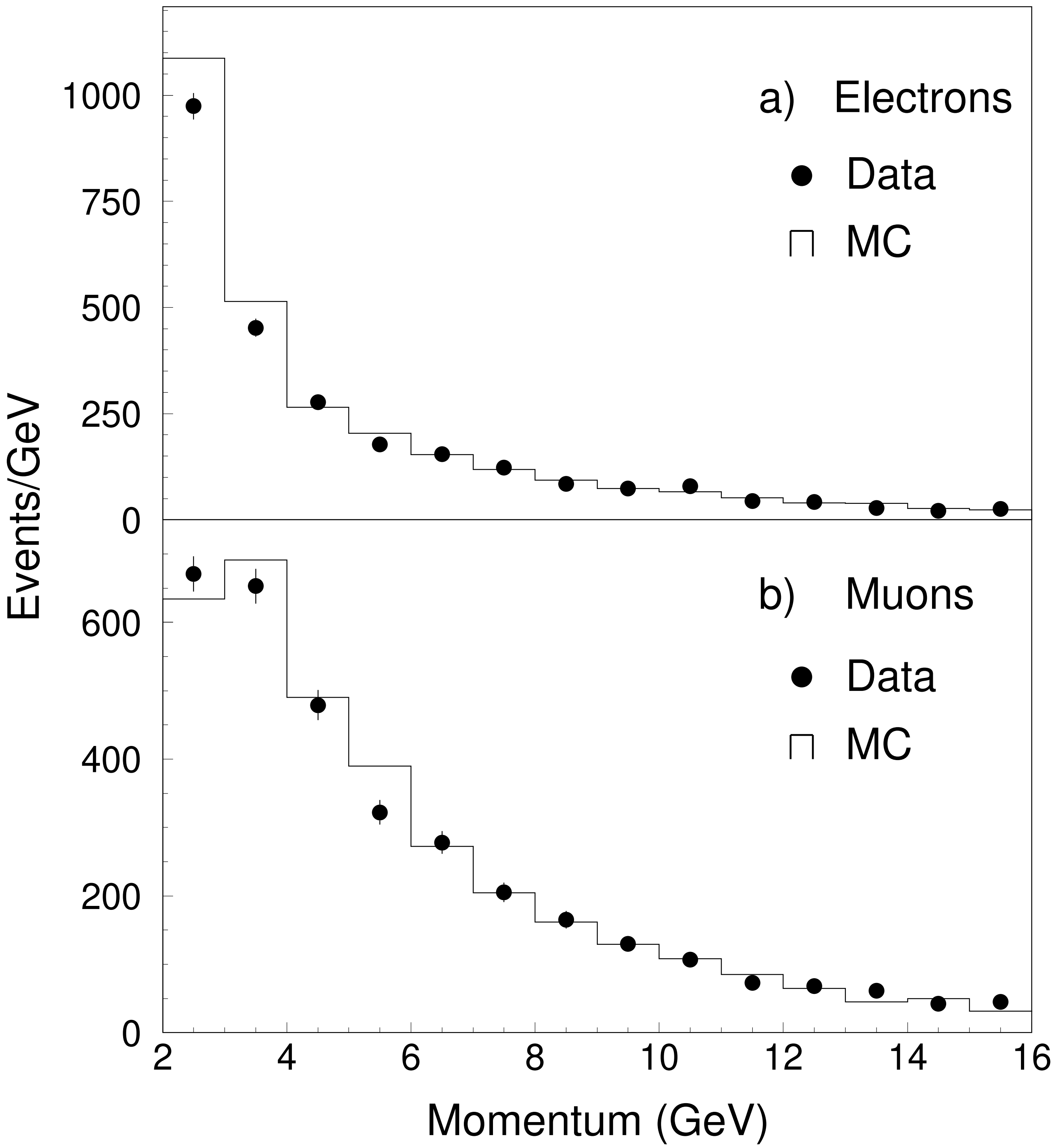
Events/GeV
1000
750
500
250
0
600
400
200
0
a) Electrons
Data
MC
b) Muons
Data
MC
2
4
6
8
10
12
14
16
Momentum (GeV)

Figure 1

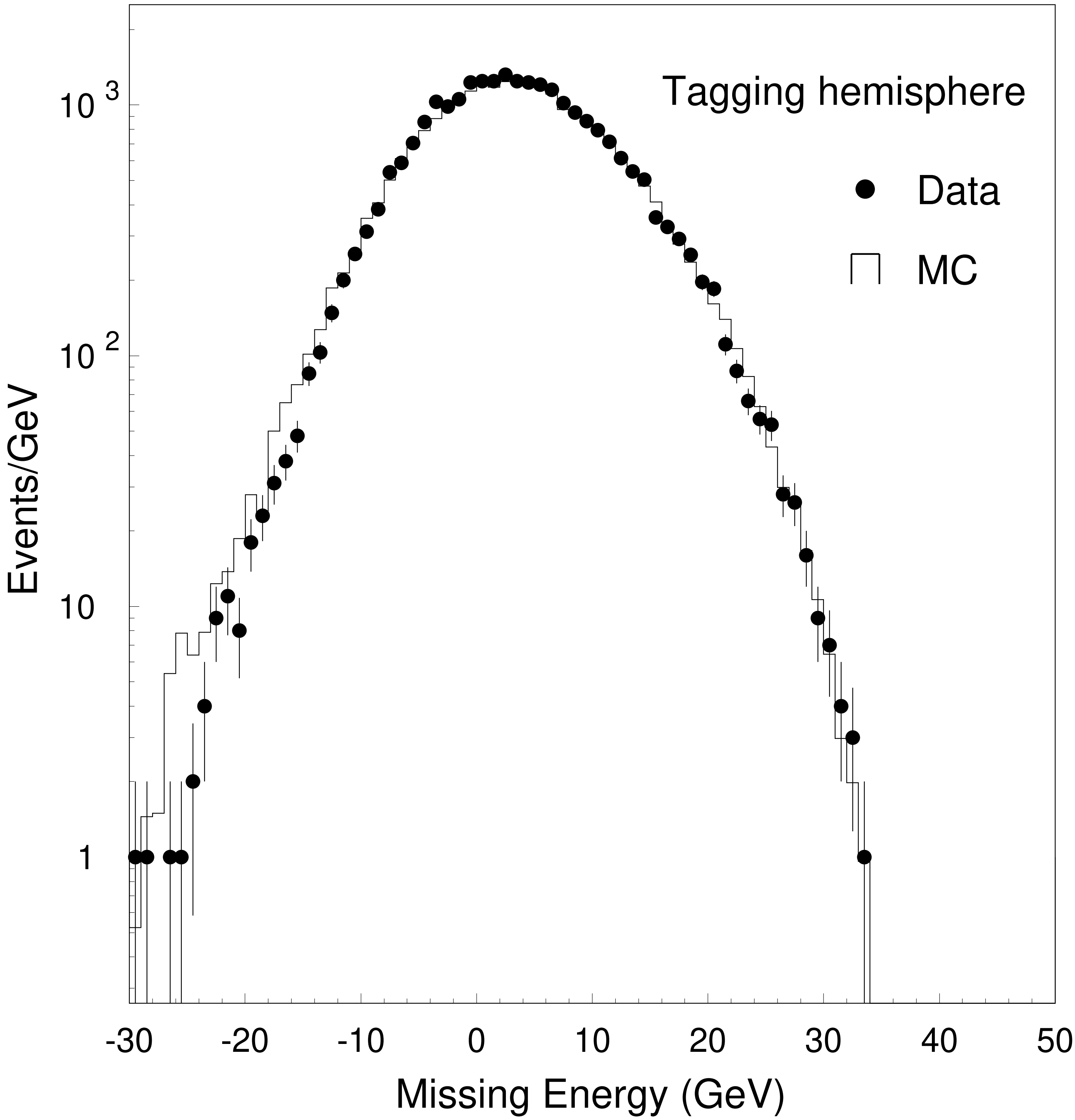
Tagging hemisphere
Data
MC
Events/GeV
10^3
10^2
10
1
-30
-20
-10
0
10
20
30
40
50
Missing Energy (GeV)

Figure 2

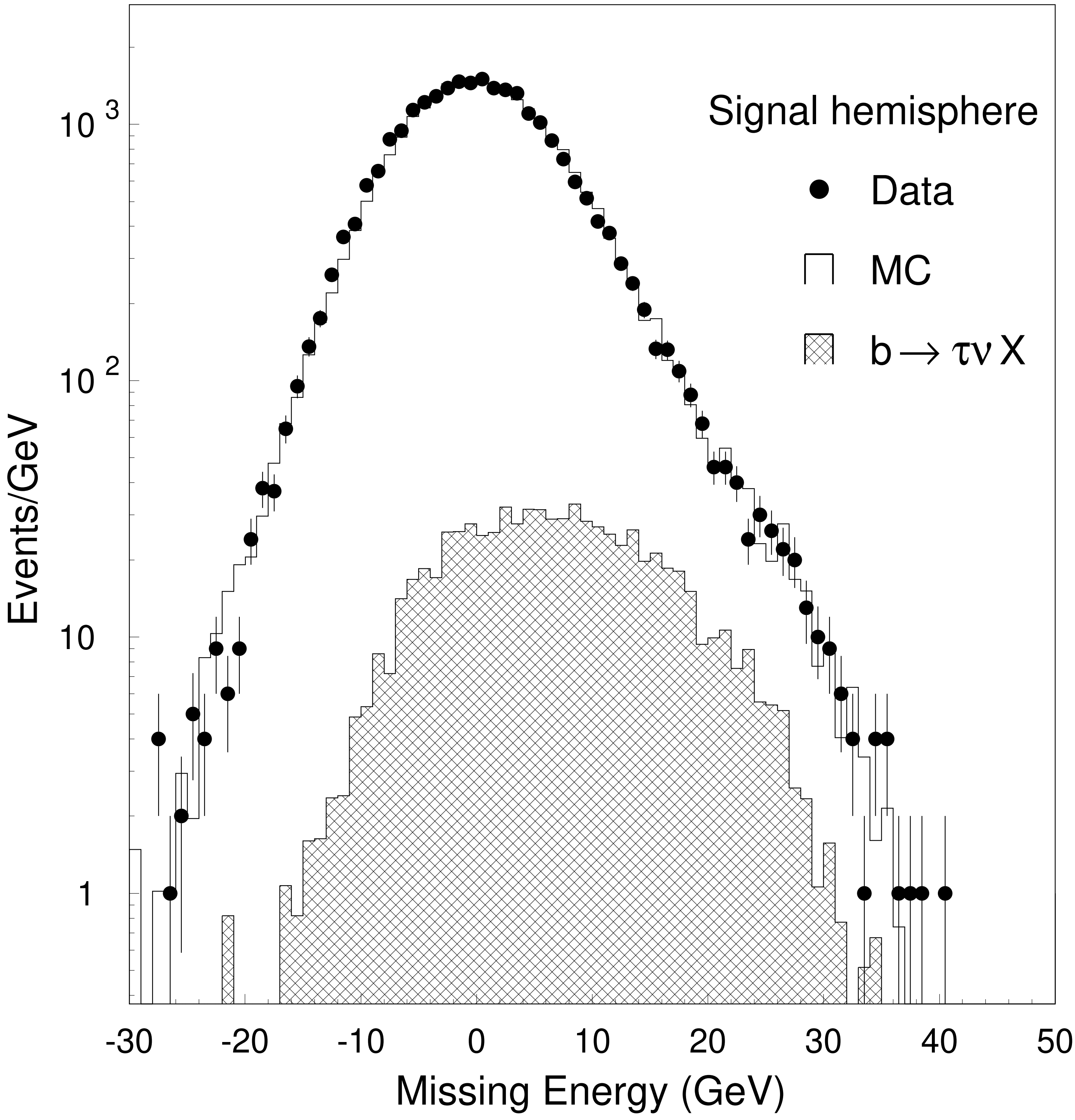
Signal hemisphere
Data
MC
$b \to \tau\nu X$
Events/GeV
Missing Energy (GeV)
10^3
10^2
10
1
-30
-20
-10
0
10
20
30
40
50

Figure 3

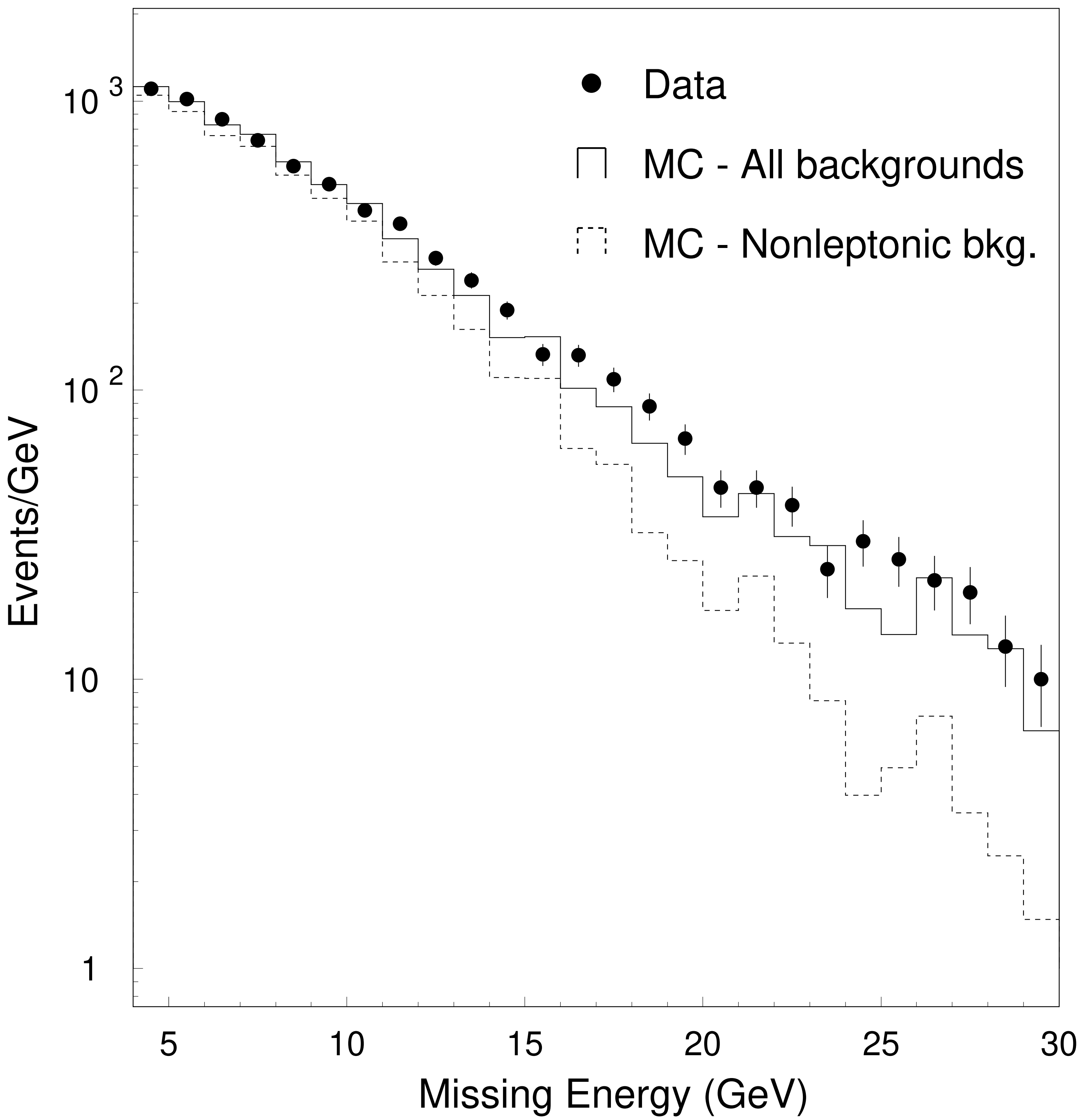
Data
MC - All backgrounds
MC - Nonleptonic bkg.
Events/GeV
10^3
10^2
10
1
5
10
15
20
25
30
Missing Energy (GeV)

Figure 4